PHYSICAL REVIEW D **89,** 083532 (2014)

Dark matter production in late time reheating

Keisuke Harigaya,[1] Masahiro Kawasaki,[2,1] Kyohei Mukaida,[3] and Masaki Yamada[1,2]
[1]*Kavli IPMU (WPI), TODIAS, University of Tokyo, Kashiwa 277-8583, Japan*
[2]*ICRR, University of Tokyo, Kashiwa 277-8582, Japan*
[3]*Department of Physics, Faculty of Science, University of Tokyo, Bunkyo-ku 133-0033, Japan*
(Received 27 February 2014; published 23 April 2014)

We estimate dark matter (DM) density for the Universe with a reheating temperature smaller than the mass of DM, assuming DM to be a weakly interacting massive particle. During the reheating process, an inflaton decays and releases high-energy particles, which are scattered inelastically by the thermal plasma and emit many particles. DMs are produced through these inelastic scattering processes and pair creation processes by high-energy particles. We properly take account of the Landau-Pomeranchuk-Migdal effect on inelastic processes and show that the resultant energy density of DM is much larger than that estimated in the literature and can be consistent with that observed when the mass of DM is larger than $O(100)$ GeV.

DOI: 10.1103/PhysRevD.89.083532 PACS numbers: 98.80.Cq, 12.60.Jv, 95.35.+d

I. INTRODUCTION

A weakly interacting massive particle (WIMP) is one of the most attractive candidates for dark matter (DM), motivated by new physics at a TeV scale, including supersymmetric (SUSY) theories. DM is produced thermally in the early Universe, and its abundance can be consistent with that observed if the reheating temperature of the Universe is sufficiently larger than its freeze-out temperature. The coincidence of the observed DM density and the relic density determined by the weak interaction scale is referred to as the WIMP miracle. Since this scenario requires the mass of the WIMP at the electroweak or TeV scale, there are rich implications for near-future experiments, including direct and indirect detection experiments of DM and particle collider experiments.

However, when we look at each model motivated by particle physics, it is nontrivial to obtain a correct mass spectrum that can account for the abundance of DM. For example, in the constrained minimal SUSY standard model, the lightest SUSY particle (LSP) is binolike. Nonobservation of SUSY particles and the discovery of the 126-GeV Higgs boson [1,2] by the LHC experiment indicate that SUSY particles are heavy, which leads to overproduction of the binolike LSP in the early Universe.[1] Taking this situation seriously, we reconsider the assumption of high reheating temperature.

When we consider inflationary models, a scenario with a low reheating temperature is naturally realized as follows. The inflaton is required to have a very flat potential, which suggests some symmetry to control its potential. The symmetry naturally suppresses interactions of the inflaton, which in turn leads to a low reheating temperature of the Universe. For example, if the mass of the inflaton is of the order of 10^{11} GeV and it decays through a dimension 6 Planck-suppressed operator, the reheating temperature of the Universe is less than about $O(1)$ GeV, which is smaller than typical freeze-out temperatures of WIMPs.

In a scenario with low reheating temperature, the thermal abundance of DM is much less than a scenario with a high reheating temperature, mainly because the energy density of the thermal plasma is a subdominant component of that of the Universe at the time of DM freeze-out [12,13]. In other words, the thermal abundance of DM is diluted by the entropy production from the inflaton decay.

However, the entropy production itself provides DM [14–19]. In Ref. [18], they have indicated that DM is produced in a shower from the decay of the inflaton and have calculated the resultant DM energy density using generalized Dokshitzer-Gribov-Lipatov-Altarelli-Parisi (DGLAP) equations [20,21] in a certain SUSY model. They have found that DM is produced efficiently through this process when the inflaton decays into particles carrying a nonzero $\mathrm{SU}(3)_c$ charge. The DM abundance also depends on the mass of inflaton, and the number of DM produced per one inflaton decay is typically $O(100)$ for the inflaton mass of $O(10^{12})$ GeV. In addition, in Ref. [19], it has been pointed out that DM is produced by inelastic scatterings between the thermal plasma and high-energy particles produced by the inflaton decay.

Therefore, in a scenario with low reheating temperature, the total amount of DM is given by the sum of the following contributions: (suppressed) thermal production, production through a cascade shower from the inflaton decay, and production through inelastic scatterings between high-energy particles and the thermal plasma. The last contribution is closely related to thermalization processes in the era of reheating, which has to be investigated in detail.

[1]This problem can be avoided by coannihilation [3,4] with the stau [5], but only with fine-tuning. For recent discussion on SUSY models with a correct DM abundance, see Refs. [6–11], for example.

When reheating temperature is low enough, the typical momentum of particles produced by the decay of inflaton, which is roughly given by the mass of the inflaton, is much larger than the (would-be) temperature of background plasma. In this case, the thermalization process is completed by splitting processes through which the number of high-energy particles drastically increases [22,23] (see also Refs. [24–26]). The rate of splitting processes is suppressed by the Landau-Pomeranchuk-Migdal (LPM) effect, which is a destructive interference effect between emission processes [27–33]. The increases in the number of high-energy particles as well as the LPM effect should be taken into account in the estimation of the DM abundance produced through inelastic processes.

In this paper, we calculate the abundance of DM produced from inelastic scatterings between high-energy particles and the thermal plasma with careful consideration on the thermalization process as mentioned above. The resultant DM abundance is independent of the mass of the inflaton as long as the mass is sufficiently large and depends mainly on the mass scale of the DM sector and reheating temperature. We find that this is the dominant contribution to the amount of DM in a scenario with a low reheating temperature when the mass of the inflaton is sufficiently large. We should emphasize that this mechanism to produce DM is highly model independent. Even if the decay channel of the inflaton into DM is absent in particular, DM is produced through inelastic scatterings. In addition, this scenario can also account for the abundance of DM with mass of $O(1)$ PeV, which is larger than unitarity bound of a few hundred TeV [34]. Such heavy DM might account for the recent observation of high-energy cosmic-ray neutrinos by the IceCube experiment [35–38].

This paper is organized as follows. In the next section, we explain how high-energy particles lose their energy in the thermal plasma taking account of the LPM effect. We also describe a thermal history of the Universe in our setup. In Sec. III, we briefly review previous works for the thermal and nonthermal production of DM and improve the calculation of the DM abundance from the inflaton decay taking account of the LPM effect. Then we discuss the relation between our scenario and other topics, such as the free-streaming velocity of DM, the Affleck-Dine baryogenesis, and SUSY theories. Section V is devoted to the conclusion.

II. THERMALIZATION AND THERMAL HISTORY

In this section, we consider a situation in which the inflaton with a mass of m_ϕ decays into light particles and the light particles yield their energy into the thermal plasma through elastic and inelastic scatterings. In Sec. II A, we calculate the rate of energy loss by elastic and inelastic scatterings, taking the LPM effect into account, and show that inelastic scatterings are the dominant process for the energy loss. In Sec. II B, we explain the evolution of the thermal plasma in the expanding universe with low reheating temperature.

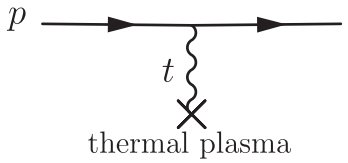

FIG. 1. Sample diagram describing an elastic scattering.

A. Interactions between high-energy particles and thermal plasma

In this subsection, we review thermalization processes of a high-energy particle with energy E_i in the thermal plasma with a low temperature $T\,(\ll E_i)$. The thermalization occurs through elastic and inelastic scatterings between a high-energy particle and the thermal plasma.

First, let us consider elastic scattering processes. Figure 1 is one of the Feynman diagrams of elastic scattering processes. When the exchanged particle is a gauge boson, the scattering cross section is dominated by the t-channel gauge boson exchange and is given as

$$\sigma_{\rm elastic} \sim \frac{\alpha^2}{t} \sim \frac{\alpha}{T^2}, \tag{1}$$

where t is one of the Mandelstam variables and α is the fine-structure constant of the gauge interaction. Although this cross section has an infrared divergence at zero temperature, an infrared cutoff arises due to a nonzero mass of the internal gauge boson at finite temperature and as large as $\alpha^{1/2}T$.[2] The rate of elastic scatterings is thus given as

$$\Gamma_{\rm el} = \langle \sigma_{\rm elastic} n \rangle \sim \alpha T, \tag{2}$$

where $\langle\rangle$ represents a thermal average and $n\,(\sim T^3)$ is the number density of scattered particles in the thermal plasma. Since the high-energy particle loses its energy by αT for each elastic scattering, the energy loss rate by elastic scatterings is estimated as

$$\left.\frac{{\rm d}E}{{\rm d}t}\right|_{\rm elastic} \sim \alpha T \langle \sigma_{\rm elastic} n \rangle \sim \alpha^2 T^2. \tag{3}$$

[2]Strictly speaking, the total cross section still has a logarithmic divergence since the almost static magnetic fields are not screened perturbatively. In the following discussion, we omit such logarithmic factors since they only change interaction rates weakly.

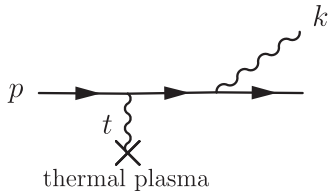

FIG. 2. Sample diagram describing an inelastic scattering.

Inelastic scattering cross sections are also dominated by t-channel contributions, as shown in Fig. 2. Since the intermediate fields are almost on shell (i.e., $t \sim \alpha T^2 \ll E_i^2$), this process can be regarded as an emission associated with an elastic scattering process. The cross section is thus given as

$$\sigma_{\rm inelastic} \sim \alpha \sigma_{\rm elastic} \sim \frac{\alpha^2}{T^2}, \tag{4}$$

where we implicitly assume that daughter particles are massless. One may consider that the rate of the splitting process is simply given by $\langle \sigma_{\rm inelastic} n \rangle$. However, we have to take account of an interference effect among emission processes, known as the LPM effect [27–33]. As we show below, the rate of inelastic processes is in fact affected and suppressed by the LPM effect.

Here, we briefly explain how the interference and suppression for inelastic scatterings occur, following Ref. [29]. Let us consider classical electrodynamics as an illustration. We assume that a classical particle with a charge e is scattered n times at x_i^μ $(i = 1, 2, ..., n)$ and changes its momentum from p_{i-1}^μ to p_i^μ by each scattering. The current density in that process is calculated from

$$j^\mu(x) = e \int {\rm d}t \frac{{\rm d}y^\mu(t)}{{\rm d}t} \delta^4(x - y(t)), \tag{5}$$

where t is the time variable. The trajectory $y(t)$ is written as

$$y^\mu(t) = x_i^\mu + \frac{p_i^\mu}{p_i^0}(t - x_i^0) \quad \text{for } x_i^0 < t < x_{i+1}^0. \tag{6}$$

The Fourier transform of the current density is thus given as

$$j^\mu(k) = ie \sum_{i=1}^{n} e^{ikx_i} \left(\frac{p_i^\mu}{kp_i} - \frac{p_{i-1}^\mu}{kp_{i-1}} \right). \tag{7}$$

The spectrum of photons radiated during scatterings is calculated from

$$\frac{{\rm d}^3 n_\gamma}{{\rm d}k^3} = -\frac{|j(k)|^2}{2k^0(2\pi)^3}. \tag{8}$$

The incoherent limit $k(x_i - x_j) \gg 1$ corresponds to the usual Bethe-Heitler limit, in which each scattering can be regarded as an independent inelastic scattering process. On the other hand, in the limit of $k(x_i - x_j) \ll 1$, adjacent terms in Eq. (7) are canceled with each other, and the radiations are suppressed. This is a physical origin of the LPM effect. The LPM effect is thus interpreted as an interference effect between a parent particle and a daughter particle, which is emitted collinearly. Although we consider the case of classical electrodynamics as an illustration, it has been proven that the same suppression effect is realized in quantum field theories, including QED and QCD [27–33].

When we write the position vector of a parent particle as $x^\mu = (\Delta t, \Delta t \hat{z})$, the interference effect remains until the phase factor varies significantly as[3]

$$1 \lesssim kx \sim \Delta t k^0 \theta^2 \sim \Delta t k_\perp^2 / k^0, \tag{9}$$

where $k_\perp$ is the perpendicular momentum of the daughter particle and $\theta\,(= k_\perp/k^0)$ is the emission angle of the daughter particle. Subsequent inelastic scattering processes are suppressed until this condition is satisfied, and thus, the inelastic scattering rate per daughter momentum is suppressed by a factor of $1/n_{\rm min} \sim 1/\Delta t \Gamma_{\rm el}$, where $n_{\rm min}$ is the lowest number of elastic scatterings to avoid the interference effect. In summary, the inelastic scattering rate is determined as

$$\Gamma_{\rm inelastic} \sim \min \left[\langle \sigma_{\rm inelastic} n \rangle, \int \frac{{\rm d}k^0}{k^0} \frac{\alpha}{\Delta t(k^0)} \right], \tag{10}$$

where $\Delta t(k^0) \sim k^0/k_\perp^2$. The first and second terms in this equation correspond to the limit of $k(x_i - x_j) \gg 1$ and $k(x_i - x_j) \ll 1$, respectively. This is the correct inelastic scattering rate with the LPM effect taken into account.

We need to estimate $\Delta t\,(\sim k^0/k_\perp^2)$ in order to determine the inelastic scattering rate given in Eq. (10). If we could neglect subsequent scatterings for the daughter particle, its perpendicular momentum is given as $k_\perp \sim \alpha^{1/2} T$. In this case, Δt is given as

[3]In the last equation, we assume that the angle θ varies dominantly by the change of direction of the daughter particle. However, since the parent particle also changes its direction due to the elastic scatterings, it contributes to the angle as $\theta \simeq p_\perp/p^0$. In fact, in the case of photon emissions, for example, this effect dominates the time scale of LPM suppression, and it is given by

$$\Delta t \sim \frac{1}{\alpha T} \left(\frac{E_i^2}{k^0 T} \right)^{1/2}.$$

However, the conclusion in this subsection and calculations in the subsequent sections are unchanged even in this case because the parent particle similarly loses its energy dominantly through a splitting into daughter particles with $k^0 \sim E_i/2$.

$$\Delta t \sim \frac{k^0}{\alpha T^2}. \tag{11}$$

When we take account of soft elastic scatterings for the daughter particle, its perpendicular momentum evolves as random walk and is described as

$$(\Delta k_\perp)^2 \sim \hat{q}_{\rm el} t, \tag{12}$$

where $\hat{q}_{\rm el}$ is a diffusion constant written by the soft elastic scattering rate for the daughter particle as

$$\hat{q}_{\rm el} \sim \int {\rm d}^2 q_\perp \frac{\partial \Gamma_{\rm el}}{\partial q_\perp^2} q_\perp^2 \sim \alpha^2 T^3. \tag{13}$$

Using these equations, we obtain

$$\Delta t \sim \left(\frac{k^0}{\hat{q}_{el}}\right)^{1/2} \sim \frac{1}{\alpha T}\left(\frac{k^0}{T}\right)^{1/2}. \tag{14}$$

Since Δt in Eq. (11) is larger than the one in Eq. (14), the latter one determines the time when the LPM effect becomes irrelevant. The rate of inelastic scatterings is therefore determined by Eqs. (10) and (14).

Taking into account the LPM effect, we obtain the rate of energy loss through inelastic scattering processes as

$$\left.\frac{{\rm d}E}{{\rm d}t}\right|_{\rm inelastic} \sim \int^{E_i/2} {\rm d}k^0 \frac{\alpha}{\Delta t(k^0)} \sim \alpha^2 T^2 \sqrt{\frac{E_i}{T}}. \tag{15}$$

Since this rate is larger than the rate of energy loss through elastic scatterings given by Eq. (3) for high-energy particles with $E_i \gg T$, they lose their energy mainly by inelastic scatterings. Note that the energy loss rate of inelastic scatterings per daughter momentum is larger for larger daughter momentum. Therefore, high-energy particles most efficiently lose their energy by a splitting into two particles with the energy of order $E_i/2$. The daughter particles continue to split, and their number density grows exponentially.

B. Thermal history

In this subsection, we briefly explain the evolution of the thermal plasma during the reheating process using the scattering rate derived in the previous subsection. For a more detailed discussion, see Ref. [23] (also Refs. [22,24–26]).

After inflation, the energy density of the Universe is dominated by an oscillating inflaton and decreases as a^{-3}, where a is the scale factor of the Universe. The inflaton decays into radiation, which is a starting point of reheating of the Universe. Let us write the mass and the decay rate of the inflaton as m_ϕ and Γ_ϕ, respectively. Daughter particles produced from inflaton decay have very high energy of the order of m_ϕ, and the number density of them, n_h, is given as

$$n_h(t) \simeq \int_t {\rm d}t' n_\phi(t')\Gamma_\phi \sim n_\phi(t)\Gamma_\phi t \sim \frac{\Gamma_\phi M_{\rm Pl}^2}{m_\phi t}, \tag{16}$$

for $\Gamma_\phi \ll H$, where H is the Hubble parameter. At the early stage of reheating, inelastic scatterings between high-energy particles generate many low-energy particles almost without losing their energy. Soon after that, low-energy particles thermalize by their own interaction, and the number density of particles in the thermal plasma is larger than that of high-energy particles at the same time. However, the energy density of radiation is still dominantly stored by high-energy particles with momentum m_ϕ, which is not thermalized yet. Eventually, high-energy particles lose their energy via inelastic scattering processes with the thermal plasma, which is the bottleneck process of thermalization in this case. We define a momentum $k_{\rm split}$ such that particles with the momentum $k_{\rm split}$ lose their energy completely and are thermalized by the time of H^{-1}. Once a splitting of a momentum k becomes efficient, a particle with a momentum smaller than k loses its energy rapidly by splitting processes. Therefore, $k_{\rm split}$ is given by

$$\frac{{\rm d}\Gamma_{\rm inelastic}}{{\rm d}\log k^0}(k_{\rm split}) \sim H. \tag{17}$$

High-energy particles efficiently supply their energy into the thermal plasma by emitting particles with the momentum $k_{\rm split}$. Since the energy conservation implies $T^4 \sim k_{\rm split} n_h$, we obtain

$$T \sim \alpha^4 \left(\frac{\Gamma_\phi M_{\rm Pl}^2}{m_\phi^3}\right) m_\phi (m_\phi t), \tag{18}$$

$$k_{\rm split} \sim \alpha^{16} \left(\frac{\Gamma_\phi M_{\rm Pl}^2}{m_\phi^3}\right)^3 m_\phi (m_\phi t)^5. \tag{19}$$

Each high-energy particle completely loses its energy when the splitting momentum becomes comparable to the maximum momentum: $k_{\rm split} \sim m_\phi$. Thermalization of high-energy particles is thus completed at the time given as

$$(m_\phi t_{\rm th}) \sim \alpha^{-16/5} \left(\frac{\Gamma_\phi M_{\rm Pl}^2}{m_\phi^3}\right)^{-3/5}. \tag{20}$$

This is the time when the temperature of the Universe is maximum:

$$T_{\rm max} \sim \alpha^{4/5} \left(\frac{\Gamma_\phi M_{\rm Pl}^2}{m_\phi^3}\right)^{2/5} m_\phi. \tag{21}$$

Note that the energy density of the Universe is still dominated by that of the inflaton.

Until the Hubble parameter becomes comparable to the decay rate of the inflaton (i.e., $H > \Gamma_\phi$), the energy density

of the Universe is still dominated by that of the inflaton. Thus, we obtain the following approximation during $t \lesssim \Gamma_\phi^{-1}$:

$$\rho_\phi \simeq \frac{4M_{\rm Pl}^2}{3t^2}, \tag{22}$$

$$H \simeq \frac{2}{3t}, \tag{23}$$

$$\rho_{\rm r} \simeq \frac{3}{5}\rho_\phi \Gamma_\phi t \simeq \frac{4\Gamma_\phi M_{\rm Pl}^2}{5t}. \tag{24}$$

After the time of $t_{\rm th}$, high-energy particles from inflaton decay are thermalized soon, and thus, the energy density of radiation $\rho_{\rm r}$ is simply characterized by the temperature T. From the last relation, we obtain the temperature of radiation as

$$T \simeq \left(\frac{36H\Gamma_\phi M_{\rm Pl}^2}{g_*(T)\pi^2}\right)^{1/4} \propto a^{-3/8}, \tag{25}$$

where g_* is the effective number of relativistic degrees of freedom.

We define reheating temperature $T_{\rm RH}$ as the temperature at which the energy density of the inflaton and radiation are equal to each other. The reheating temperature is thus obtained from the equation $H \simeq \Gamma_\phi$ and is given as

$$T_{\rm RH} \simeq \left(\frac{90}{g_*(T_{\rm RH})\pi^2}\right)^{1/4} \sqrt{\Gamma_\phi M_{\rm Pl}}. \tag{26}$$

After the era of reheating, the energy density of the Universe is dominated by that of radiation and decreases as $\propto a^{-4}$.

III. DM PRODUCTION MECHANISMS

In this section, we discuss DM production for a theory with the inflaton mass m_ϕ, the WIMP (DM) mass $m_{\rm DM}$ ($\ll m_\phi$), and a low reheating temperature $T_{\rm RH}$ ($\ll m_{\rm DM}$). We explain three mechanisms to produce DM: thermal production (Sec. III A), production through a cascade shower from inflaton decay (Sec. III B), and production through inelastic scatterings between high-energy particles and the thermal plasma (Sec. III C). These mechanisms are additional contributions with each other, and thus, the predicted DM density is the sum of these contributions in a scenario with low reheating temperature.

A. Thermal production

In this subsection, we explain thermal production of DM in the Universe with low reheating temperature. Even if $T_{\rm RH} \ll m_{\rm DM}$, DM is generated thermally during the inflaton-dominated era [12,13]. The condition to generate DM thermally is given as $T_{\rm max} \gtrsim m_{\rm DM}$, where $T_{\rm max}$ is the maximum temperature of the Universe derived as Eq. (21) and is rewritten in terms of $T_{\rm RH}$ and m_ϕ as

$$T_{\rm max} \sim \left(\alpha^2 \frac{T_{\rm RH}^2 M_{\rm Pl}}{m_\phi^3}\right)^{2/5} m_\phi, \tag{27}$$

where we use Eq. (26) and omit $O(1)$ factors. If $T_{\rm max} \ll m_{\rm DM}$, the DM density is exponentially suppressed. In the following, we calculate the DM density for the case of $T_{\rm max} \gtrsim m_{\rm DM}$ ($\gg T_{\rm RH}$).

As is the case with typical WIMP scenarios, we assume that DM has an odd Z_2 parity and thus is stable and has the weak interaction.[4] We express its thermal-averaged annihilation cross section as

$$\langle \sigma_{\rm ann} v \rangle \equiv \frac{\alpha_w}{m_{\rm DM}^2}\left(c_s + \frac{T}{m_{\rm DM}} c_p\right), \tag{28}$$

where α_w is the fine-structure constant of the weak interaction. The terms with the coefficients c_s and c_p describe the s-wave and p-wave contributions in a non-relativistic expansion of the cross section.

The number density of DM decreases through the annihilation and the Hubble expansion. Since the rate of the annihilation is proportional to the number density of DM, the annihilation process becomes irrelevant, and the number density freezes out when the following condition is satisfied:

$$n_{\rm DM}^{\rm eq}(T_F)\langle \sigma_{\rm ann} v \rangle \simeq H(T_F), \tag{29}$$

where $n_{\rm DM}^{\rm eq}$ is the number density of DM with the assumption of thermal equilibrium. Since we consider the case of $T_{\rm RH} \ll m_{\rm DM}(\sim T_F)$, DM decouples from the thermal plasma during the inflaton-dominated era, in which the temperature of the thermal plasma obeys Eq. (25). Defining $x_F \equiv m_{\rm DM}/T_F$, we rewrite the condition (29) as

$$x_F \simeq \log\left[\frac{6}{\sqrt{5}\pi^{5/2}} \frac{g_*^{1/2}(T_{\rm RH})}{g_*(T_F)} \frac{M_{\rm Pl}}{m_{\rm DM}} \times \alpha_w \left(c_s + \frac{5}{4} c_p x_F^{-1}\right) x_F^{1/2} \frac{T_{\rm RH}^2}{T_F^2}\right]. \tag{30}$$

The DM freeze-out occurs earlier compared with the ordinary case of thermal production of DM roughly by a factor of $\log[T_{\rm RH}^2/T_F^2]$. This is because the energy density of radiation is less than that of inflaton during the inflaton-dominated era, and the expansion rate of the Universe

[4] If DM interacts with Standard Model (SM) particles only through a heavy mediator or a higher dimensional interaction so that DM has never been in thermal equilibrium, DM is non-thermally produced mainly around the end of the reheating [39–43].

evolves faster than in the ordinary case. We obtain the abundance of DM as

$$n_{\rm DM}|_{T=T_F} \simeq \frac{2m_{\rm DM}^3}{(2\pi x_F)^{3/2}} e^{-x_F}. \tag{31}$$

Here we comment on the case of $m_{\rm DM} \gtrsim (T_{\rm RH}^2 M_{\rm Pl})^{1/3}$. In this case, DM never reaches the chemical equiliblium because the combination of $n_{\rm DM}^{\rm eq}(T)\langle\sigma_{\rm ann}v\rangle$ is always less than the Hubble parameter, $H(T)$. Since we assume $T_{\rm max} \gtrsim m_{\rm DM}$, DM is produced through a pair creation (= inverse annihilation) process. Assuming its cross section to be $\alpha_w T^{-2}$ for $T \gtrsim m_{\rm DM}$, we find that DM is dominantly produced at $T = m_{\rm DM}$ and obtain its abundance as

$$n_{\rm DM}|_{T=m_{\rm DM}} \simeq \frac{(n_{\rm DM}^{\rm eq})^2_{T=m_{\rm DM}}\langle\sigma_{\rm ann}v\rangle}{H(T=m_{\rm DM})}, \tag{32}$$

$$\simeq \frac{9\zeta^2(3)}{\sqrt{10}\pi^5}\frac{\alpha_w g_*^{1/2}(T_{\rm RH})}{g_*(m_{\rm DM})} M_{\rm Pl} T_{\rm RH}^2 \quad \text{for } m_{\rm DM} \gtrsim (T_{\rm RH}^2 M_{\rm Pl})^{1/3}, \tag{33}$$

where $\zeta(3) \simeq 1.20205\ldots$ is the Riemann zeta function.

The present energy density of DM from the thermal production divided by the entropy density of the Universe is thus given as

$$\left.\frac{\rho_{\rm DM}^{\rm th}}{s}\right|_{\rm now} \simeq \left.\frac{3T_{\rm RH}\rho_{\rm DM}^{\rm th}}{4\rho_\phi}\right|_{\rm RH}, \tag{34}$$

$$\simeq \left.\frac{3T_{\rm RH}\rho_{\rm DM}^{\rm th}}{4\rho_\phi}\right|_{\rm F}, \tag{35}$$

$$\simeq \left.\frac{\rho_{\rm DM}^{\rm th}}{s}\right|_{\rm F}\left(\frac{T_{\rm RH}\rho_r}{T_F\rho_\phi}\right)_F, \tag{36}$$

$$\simeq \left.\frac{\rho_{\rm DM}^{\rm th}}{s}\right|_{\rm F}\left(\frac{T_{\rm RH}}{T_{\rm F}}\right)^5, \tag{37}$$

where the subscripts RH and F represent the corresponding value at the time of reheating and DM freeze-out, respectively. We use $s = 4\rho_{\rm r}/3T$ in the first and third lines, $\rho_{\rm DM}^{\rm th} \propto \rho_\phi \propto a^{-3}$ in the second line, and $T \propto a^{-3/8}$ in the last line. The DM abundance is suppressed compared with the ordinary case of thermal production of DM due to the entropy production from the inflaton decay after the time of DM freeze-out. This scenario has been considered in the literature in order to suppress the abundance of WIMPs with relatively large mass [12,13].

B. DM production through cascade shower from inflaton decay

DM may be directly produced by the decay of the inflaton [14–17]. The number density of DM from this contribution at the temperature $T = T_{\rm RH}$ is given as

$$n_{\rm DM}^{\rm dir}|_{T=T_{\rm RH}} = {\rm Br}(\phi \to {\rm DM}) n_\phi|_{T=T_{\rm RH}}, \tag{38}$$

where n_ϕ is the number density of the inflaton. We denote the branching ratio of inflaton decay into DM as ${\rm Br}(\phi \to {\rm DM})$, which depends on the model one considers. For example, ${\rm Br}(\phi \to {\rm DM}) = O(1)$ in SUSY theories due to SUSY and the R-parity conservation. From Eq. (38), one may estimate the DM abundance from the decay of the inflaton at the present time as

$$\left.\frac{n_{\rm DM}^{\rm dir}}{s}\right|_{\rm now} \simeq T_{\rm RH}\left.\frac{3n_{\rm DM}^{\rm dir}}{4\rho_\phi}\right|_{T=T_{\rm RH}}, \tag{39}$$

$$\simeq \frac{3T_{\rm RH}}{4m_\phi}{\rm Br}(\phi \to {\rm DM}). \tag{40}$$

However, we have to take account of the contribution from the cascade decay of the inflaton. This has been investigated in Ref. [18], where they assume the minimal SUSY standard model. Using generalized DGLAP equations [20,21], they have found that more than one DM (LSP, in that paper) is produced through each cascade decay of the inflaton. Their results are written as

$$\left.\frac{n_{\rm DM}^{\rm shower}}{s}\right|_{\rm now} \simeq \frac{3T_{\rm RH}}{4m_\phi}\sum_i {\rm Br}(\phi \to i)\nu_i, \tag{41}$$

where ν_i is the averaged number of DM in a shower produced by a primary particle i. The factor ν_i increases with increasing the mass of the inflaton and strongly depends on particle species i. For example, if $m_\phi = 10^{13}$ GeV and $m_{\rm DM} = 1$ TeV, ν_i is calculated as $\mathcal{O}(1)$, $\mathcal{O}(10^2)$, and $\mathcal{O}(10)$ for (s)neutrinos, $SU(3)_c$-charged particles, and the other particles, respectively.[5]

C. DM production through inelastic scatterings

In this section, we consider inelastic scattering processes between high-energy particles and the thermal plasma. Since relevant processes are inelastic scatterings into two high-energy particles, as explained in Sec. II, we refer to those processes as splittings. We concentrate on the time when the temperature is in the interval $T_{\rm RH} < T \ll T_{\rm max}$, i.e., $\Gamma_\phi^{-1} \gtrsim t \gg t_{\rm th}$.

The inflaton decays into particles with the energy of the order of its mass m_ϕ, and the daughter particles lose their energy by splitting continuously. DM is produced with a certain rate throughout these splitting processes when the energy of the splitted particles is sufficiently large. We define a threshold energy as

[5]These results have been obtained by extrapolating data points of the inflaton mass $m_\phi \le 10^{10}$ GeV, and thus, there are some uncertainties.

$$E_{\rm th} \equiv \frac{m_{\rm DM}^2}{4T}. \tag{42}$$

When a high-energy particle has energy larger than this threshold energy, inelastic scatterings between the high-energy particle and the thermal plasma can produce DM. The cross section of a DM production process is suppressed by the mass of DM as [19]

$$\sigma_{\rm DM} \sim \max\left[\frac{\alpha_{\rm DM}^2}{s}, \frac{\alpha_{\rm DM}^3}{m_{\rm DM}^2}\right], \tag{43}$$

where s is one of the Mandelstam variables and is given by $4ET$. The former cross section is nothing but the ordinary pair creation from an annihilation of the high-energy particle and a particle in the thermal plasma. The physics behind the latter cross section is equivalent to the e^+e^- pair production from a high-energy photon interacting with a nuclei, where the cross section is proportional to the inverse of the squared electron mass. We write the fine-structure constant of DM production processes as $\alpha_{\rm DM}$, which is generally different from the one appearing in the inelastic scattering rate [see Eqs. (10) and (14)]. For a reaction with energy just above the threshold (i.e., $E \gtrsim E_{\rm th}$), which we are most interested in as explained below, the rate of the DM production process is given as

$$\Gamma_{\rm DM}\Big|_{E\sim E_{\rm th}} \sim \langle \sigma_{\rm DM} n \rangle \sim \frac{\alpha_{\rm DM}^2 T^3}{m_{\rm DM}^2}. \tag{44}$$

Note that this is so small that the LPM effect is irrelevant for this process [see Eqs. (10) and (14)], and thus, the rate of the DM production process is indeed given by this formula.

Here we estimate the number density of DM produced through inelastic scattering processes. A more detailed discussion is done in the Appendix, where we solve the Boltzmann equation describing inelastic scattering processes. Let us consider the evolution of high-energy particles. First, they are produced by the decay of the inflaton and have the energy of the order of its mass m_ϕ. Soon after that, the daughter particles split into many high-energy particles. The high-energy particles continue to split, and their number density grows exponentially. Given a certain time when their energy is of the order of E, we can estimate their number density n_h as

$$n_h \sim \frac{m_\phi}{E} n_\phi \Gamma_\phi t \quad \text{for } t_{\rm th} \ll t \lesssim \Gamma_\phi^{-1}, \tag{45}$$

from the conservation of energy. Here we use the fact that the splitting process is much faster than the decay of the inflaton since they satisfy the inequality $\Gamma_{\rm split} \gg \Gamma_\phi$ for $t_{\rm th} \ll t \lesssim \Gamma_\phi^{-1}$. Throughout these processes, DM is also produced by scatterings of high-energy particles with the rate given in Eq. (44), until they lose their energy down to $E_{\rm th}$. At a certain time when their energy is of the order of E, the number density of DM that is produced during the splitting of the high-energy particles (i.e., $\Gamma_{\rm inelastic}(E)^{-1}$) is therefore given by

$$n_{\rm DM}^{\rm sca} \sim \frac{\Gamma_{\rm DM}}{\Gamma_{\rm inelastic}} n_h \sim \frac{\alpha_{\rm DM}^2 T^3}{m_{\rm DM}^2} \frac{\sqrt{E}}{\alpha^2 T\sqrt{T}} \frac{m_\phi}{E} n_\phi \Gamma_\phi t \quad \text{for } t_{\rm th} \ll t \lesssim \Gamma_\phi^{-1}. \tag{46}$$

Equations (25) and (46) imply that the abundance of DM increases with decreasing E and T. Taking into account the inequality $m_\phi/2 \geq E_{\rm th}$, which constrains the temperature as $T \geq m_{\rm DM}^2/2m_\phi$ to produce the DM, we conclude that the energy density of the DM is given by

$$\frac{\rho_{\rm DM}^{\rm sca}}{s} \sim m_{\rm DM} \frac{\alpha_{\rm DM}^2 T^3}{m_{\rm DM}^2} \frac{\sqrt{E_{\rm th}}}{\alpha^2 T\sqrt{T}} \frac{m_\phi}{E_{\rm th}} \Gamma_\phi t\Big|_{T=\max(T_{\rm RH}, m_{\rm DM}^2/2m_\phi)} \times \frac{n_\phi}{s}\Big|_{T=T_{\rm RH}}, \tag{47}$$

$$\sim \begin{cases} \frac{\alpha_{\rm DM}^2}{\alpha^2}\frac{T_{\rm RH}^3}{m_{\rm DM}^2} & \text{for } m_\phi \geq \frac{m_{\rm DM}^2}{2T_{\rm RH}}, \\ \frac{\alpha_{\rm DM}^2}{\alpha^2}\frac{4T_{\rm RH}^5 m_\phi^2}{m_{\rm DM}^6} & \text{for } \frac{m_{\rm DM}^2}{2T_{\rm max}} \ll m_\phi < \frac{m_{\rm DM}^2}{2T_{\rm RH}}, \end{cases} \tag{48}$$

where we use Eq. (25) to express t in terms of T as $\Gamma_\phi t \sim T_{\rm RH}^4/T^4$. The first equality is justified by solving the Boltzmann equation in the Appendix. We should emphasize that this result is independent of the mass of the inflaton once the condition to produce the DM is satisfied at $T = T_{\rm RH}$ (i.e., $m_\phi \geq m_{\rm DM}^2/2T_{\rm RH}$).

In the above analysis, we assume that the thermalization of decay products proceeds through inelastic scatterings and elastic scatterings are negligible, which is the case when decay products have gauge interactions as we have shown in Sec. II A. However, when the temperature of the thermal plasma is smaller than the QCD scale, $\Lambda_{\rm QCD} = O(100)$ MeV, $\mathrm{SU}(3)_c$-charged particles hadronize. Some hadrons, such as the neutral pion, have no gauge interactions, and the energy loss by splitting processes is suppressed. Therefore, the energy loss by elastic processes is important, and the number density of high-energy particles given in Eq. (45) is overestimated for $T \lesssim \Lambda_{\rm QCD}$. Since the estimation of the number density of high-energy particles for $T \lesssim \Lambda_{\rm QCD}$ suffers from large uncertainties due to the nonperturbative feature of hadronization, we leave it for a future work.

D. Summary

The amount of DM at the present time has been observed by the Planck collaboration [44] as

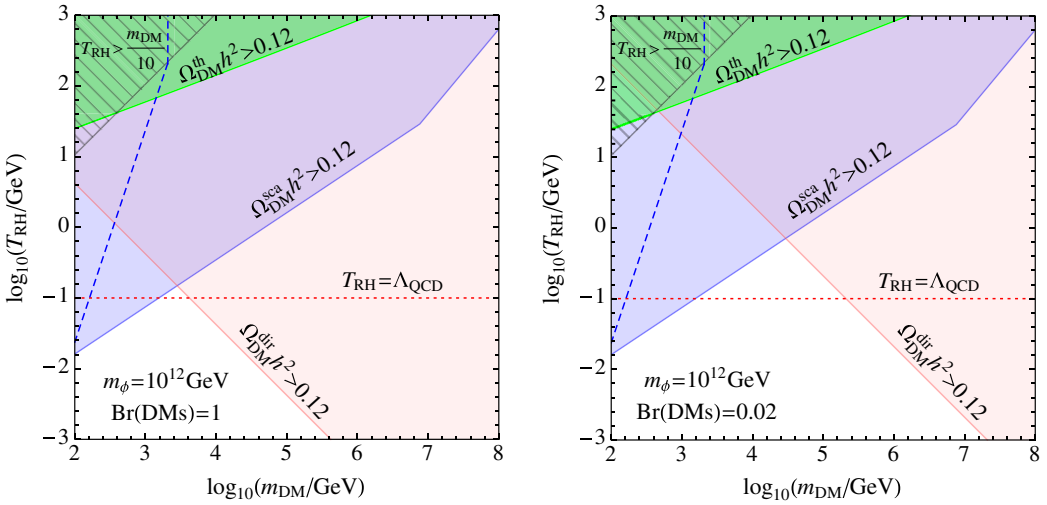

FIG. 3 (color online). Exclusion plot in a scenario with low reheating temperature. We assume that the mass of the inflaton m_ϕ is 10^{12} GeV and that the branching of inflaton decay into DM is 1 (left panel) and 0.02 (right panel). We also assume $\alpha_{\rm DM} = \alpha$. The abundance of DM produced from thermal production ($\Omega^{\rm th}_{\rm DM}h^2$), direct decay of inflaton ($\Omega^{\rm dir}_{\rm DM}h^2$), and inelastic scatterings ($\Omega^{\rm sca}_{\rm DM}h^2$) is larger than that observed in the green (dark gray), red (light gray), and blue (middle gray) shaded regions, respectively. The striped region are $T_{\rm RH} > m_{\rm DM}/10$, in which DM is produced only thermally. The abundance of DM is less than that observed above the blue dashed line due to its annihilation. Here, we have assumed that the annihilation of DM is efficient and its cross section is $10^{-2}m_{\rm DM}^{-2}$. The red dotted lines represent the reheating temperature below which $\Omega^{\rm sca}_{\rm DM}h^2$ is overestimated.

$$\Omega_{\rm DM}h^2 = 0.1196 \pm 0.0031. \tag{49}$$

Using $\Omega_{\rm DM}h^2 \simeq (\rho_{\rm DM}/s)/3.5$ eV and Eq. (48), we obtain the relation between the mass of DM and the reheating temperature as

$$m_{\rm DM} \sim 1.5\ {\rm TeV}\left(\frac{\alpha_{\rm DM}}{\alpha}\right)\left(\frac{T_{\rm RH}}{100\ {\rm MeV}}\right)^{3/2}, \tag{50}$$

once the condition of $m_\phi \geq m^2_{\rm DM}/2T_{\rm RH}$ is satisfied and the contribution from the decay of the inflaton is neglected.

Let us discuss whether the annihilation of DM is negligible or not [45] for the parameter of the interest given in Eq. (50). The annihilation of DM is irrelevant when the following condition is satisfied:

$$\frac{n_{\rm DM}\langle\sigma_{\rm ann}v\rangle}{H} \ll 1. \tag{51}$$

In the case of $m_\phi \geq m^2_{\rm DM}/2T_{\rm RH}$, the DM abundance is determined at $T = T_{\rm RH}$, and hence, the left-hand side of this inequality should be calculated at $T = T_{\rm RH}$, and we obtain an upper bound on the abundance of DM as

$$\Omega_{\rm DM}h^2 \ll \frac{1}{3.5\ {\rm eV}}\left(\frac{45}{8\pi^2 g_*(T_{\rm RH})}\right)^{1/2}\frac{m_{\rm DM}}{\langle\sigma_{\rm ann}v\rangle M_{\rm Pl}T_{\rm RH}}, \tag{52}$$

$$\simeq 10^2\left(\frac{10}{g_*(T_{\rm RH})}\right)^{1/2}\left(\frac{10^{-2}m^{-2}_{\rm DM}}{\langle\sigma_{\rm ann}v\rangle}\right) \times\left(\frac{m_{\rm DM}}{1.5\ {\rm TeV}}\right)^3\left(\frac{100\ {\rm MeV}}{T_{\rm RH}}\right). \tag{53}$$

For $m_{\rm DM}$ and $T_{\rm RH}$ given in Eq. (50), the upper bound on the DM abundance is larger than the observed DM abundance as long as $m_{\rm DM} > O(100)$ GeV.[6] Therefore, the prediction in Eq. (50) is valid for $m_{\rm DM} > O(100)$ GeV.

Figures 3 and 4 summarize the results obtained in this section. Although we take account of the production of DM from direct decay of the inflaton, we omit the contribution of the DM production from a shower of inflaton decay since it depends models and has uncertainties, as we have mentioned. We assume that $\alpha_{\rm DM} = \alpha$ and the mass of the inflaton is 10^{12} GeV and 10^{15} GeV in Figs. 3 and 4, respectively.[7] The blue (middle gray) shaded areas are regions in which the energy density of DM produced by inelastic scatterings exceeds the observed one. The boundaries of the blue (middle gray) shaded regions are thus given by Eq. (50), once the condition of $m_\phi \geq m^2_{\rm DM}/2T_{\rm RH}$ is satisfied. In the case of $m_\phi \leq m^2_{\rm DM}/2T_{\rm RH}$, which appears in the upper-right regions of Fig. 3, the abundance of DM is calculated from the second line of Eq. (48). Below the red dotted lines, the reheating temperature is smaller than the QCD scale, and the DM density is overestimated (see the comment in the last paragraph of Sec. III C). Therefore, for $m_{\rm DM} \lesssim 10^3$ GeV, the correct DM abundance is obtained at

[6]Here, we implicitly assume that DM loses its momentum just after they are produced. If that is not the case, the annihilation cross section of DM is as small as $\alpha^2 E^{-2}_{\rm th} \ll 10^{-2}m^{-2}_{\rm DM}$, and the upper bound on DM abundance can be much larger than the reference value given in Eq. (53).

[7]The inflaton mass of 10^{15} GeV is possible in models proposed in Refs. [46–48].

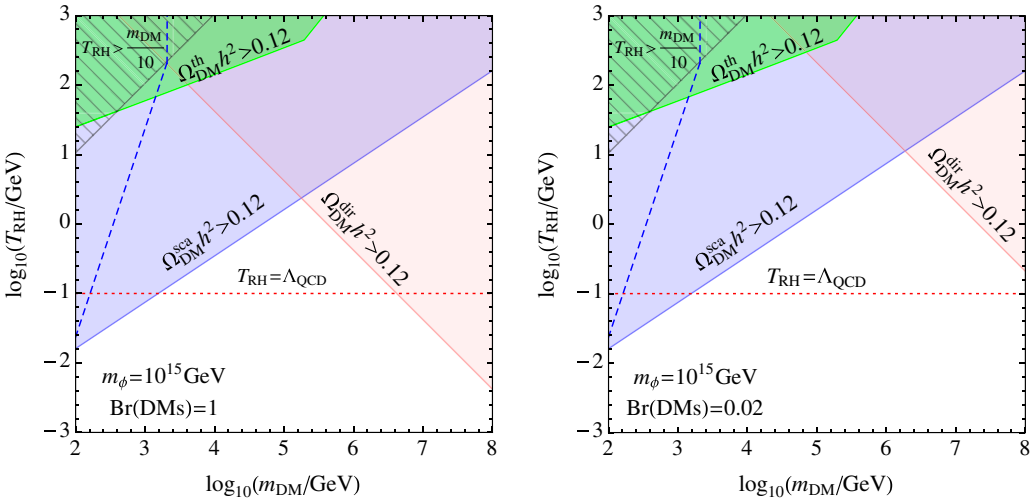

FIG. 4 (color online). Same as Fig. 3, but assuming the mass of the inflaton to be 10^{15} GeV.

a certain reheating temperature between the red dotted lines and the lower edges of the blue (middle gray) shaded regions. Given the mass of the inflaton m_ϕ and the branching ratio of inflaton decay into DM sector $\mathrm{Br}(\phi \to \mathrm{DM})$, we have an upper bound on the mass of DM above which the amount of DM from direct decay of inflaton is larger than that observed [red (light gray) shaded regions]. If the annihilation of DM is efficient and its cross section is as large as $10^{-2}m_{\mathrm{DM}}^{-2}$, the abundance of DM is equal to and less than that observed on and above the blue dashed lines, respectively. The blue dashed line in the striped regions corresponds to the conventional thermal WIMP scenario. The DM production from thermal process calculated in Sec. III A is always subdominant in these parameter regions. Note that DM with a mass of $O(1)$ PeV can account for the abundance of DM if the branching ratio of the inflaton into the DM sector is suppressed and the reheating temperature is as large as 10 GeV.

Finally, we comment on the case in which the mass of DM and the reheating temperature are within the nonshaded regions or above the blue dashed lines in Figs. 3 and 4. In this case, we need other sources of DM or other DM candidates to account for the observed DM abundance. The former solution is easily realized by the decay of long-lived matter: moduli [14–16] or Q-ball [45,49–51], for example. Axion, which is introduced by the Peccei-Quinn mechanism [52], is one of the well-motivated candidates for the latter solution.

IV. DISCUSSIONS

In this section, we discuss the relation between our result and some related topics: the free-streaming velocity of DM, Affleck-Dine baryogenesis, heavy DM with mass of $O(1)$ PeV, and SUSY theories.

A. Free-streaming velocity of DM

Since DM is relativistic after the time of DM decoupling in the low reheating temperature scenario, it might have a cosmologically relevant free-streaming velocity. If interactions between DM and the thermal plasma are negligible, the present-day free-streaming velocity of DM is calculated as

$$v_0 \simeq \frac{E_{\mathrm{th}}|_{T=T_{\mathrm{RH}}}}{m_{\mathrm{DM}}}\frac{T_0}{T_{\mathrm{RH}}}\left(\frac{g_{*s}(T_0)}{g_{*s}(T_{\mathrm{RH}})}\right)^{1/3}, \tag{54}$$

$$\simeq 8.7\times 10^{-9}\left(\frac{m_{\mathrm{DM}}}{1.5\ \mathrm{TeV}}\right)\left(\frac{T_{\mathrm{RH}}}{100\ \mathrm{MeV}}\right)^{-2}\left(\frac{g_{*s}(T_0)}{g_{*s}(T_{\mathrm{RH}})}\right)^{1/3}, \tag{55}$$

$$\sim 8.7\times 10^{-9}\left(\frac{m_{\mathrm{DM}}}{1.5\ \mathrm{TeV}}\right)^{-1/3}\left(\frac{g_{*s}(T_0)}{g_{*s}(T_{\mathrm{RH}})}\right)^{1/3}, \tag{56}$$

where $T_0\,(\simeq 2.3\times 10^{-4}\ \mathrm{eV})$ is the temperature at the present time and g_{*s} is the effective number of relativistic degrees of freedom for entropy. Here, we assume that $m_\phi \geq m_{\mathrm{DM}}^2/2T_{\mathrm{RH}}$ and use Eq. (50) in the last line. Although the observation of the Lyman-α forest constrains the free-streaming velocity as $v_0 \lesssim 2.5\times 10^{-8}$ [53] (see Ref. [54] for review), we find that the above result satisfies this constraint when $m_{\mathrm{DM}} \gtrsim 100$ GeV. The free-streaming velocity will be further constrained by future observations of the redshifted 21-cm line because the erasure of small-scale structure results in delaying star formation and thus delaying the buildup of UV and x-ray backgrounds, which affects the 21-cm radiation signal produced by neutral hydrogen. It is expected that future observations of the redshifted 21-cm line would improve the upper bound to $v_0 \lesssim 2\times 10^{-9}$ [55]. The low reheating temperature scenario with $m_{\mathrm{DM}} \lesssim 100$ TeV would be tested by future

observations of the redshifted 21-cm line. In many cases, however, we have to take into account interactions between DM and the thermal plasma and the constraint from free-streaming velocity is absent [56–58].

B. Affleck-Dine mechanism

Since the reheating temperature is very low, mechanisms to account for the baryon asymmetry of the Universe are limited. One well-motivated mechanism is the Affleck-Dine mechanism, which is naturally realized in SUSY theories [59,60]. Note that the Affleck-Dine mechanism predicts nonzero baryonic isocurvature fluctuation when Hubble-induced A terms are absent during inflation. This is indeed realized if one considers the models of D-term inflation [61–63] or if the field which has a nonzero F-term during inflation is charged under some symmetry and its vacuum expectation value is less than the Planck scale during inflation [64]. Since observations of cosmic microwave background have shown that the density perturbations are predominantly adiabatic [65,66], the isocurvature perturbation is tightly constrained. The Planck collaboration puts an upper bound as [44]

$$|S_{b\gamma}| \lesssim \frac{\Omega_{\rm DM}}{\Omega_b}(0.039 \times 2.2 \times 10^{-9})^{1/2} \simeq 5.0 \times 10^{-5}, \quad (57)$$

where $S_{b\gamma}$ is the baryonic isocurvature fluctuation and Ω_b denotes the density parameter of the baryon. This upper bound then gives a constraint as [64]

$$T_{\rm RH} \lesssim 1.1 \times 10^{-17} \frac{1}{n^2} \frac{M_{\rm Pl}^2}{m_{3/2}} \left(\frac{m_{\rm DM}}{H_{\rm inf}}\right)^{\frac{2n-6}{n-2}} \Theta, \quad (58)$$

where $m_{3/2}$ is a gravitino mass, $H_{\rm inf}$ is the Hubble parameter during inflation, and Θ is an $O(1)$ factor. Here, we assume that the Affleck-Dine field Φ has a mass of the order of $m_{\rm DM}$ and is stabilized via a superpotential term $\propto \Phi^n (n \geq 4)$. Using Eq. (50), we obtain the following constraints:

$$m_{\rm DM}\left(\frac{m_{3/2}}{m_{\rm DM}}\right)^{3/2} \lesssim 10^{14}\ {\rm GeV}\left(\frac{H_{\rm inf}}{10^{12}\ {\rm GeV}}\right)^{-3/2} \Theta^{3/2} \quad (59)$$

for $n = 4$ and

$$m_{\rm DM}\left(\frac{m_{3/2}}{m_{\rm DM}}\right)^{6} \lesssim 2 \times 10^{19}\ {\rm GeV}\left(\frac{H_{\rm inf}}{10^{12}\ {\rm GeV}}\right)^{-9} \Theta^{6} \quad (60)$$

for $n = 6$. While the Affleck-Dine baryogenesis with $n = 6$ puts the severe upper bound on the energy scale of inflation $H_{\rm inf}$, we can easily avoid this constraint for the case of $n = 4$.

C. PeV DM

It is worth noting that we can account for the abundance of DM even in the case that DM is a WIMP with a mass larger than the unitarity bound of a few hundred TeV [34]. The recent observation of high-energy cosmic-ray neutrinos by the IceCube experiment may indicate that DM is a long-lived particle with a mass of $O(1)$ PeV [35–38]. The above scenario for nonthermal production of DM can also account for the abundance of even such a heavy DM.

D. SUSY theories

SUSY models often have difficulties in obtaining the correct DM abundance. For example, in the constrained minimal SUSY standard model, the LSP is binolike in most of the parameter space, which leads to overclosure by thermally produced binos. Although this situation can be remedied by coannihilation [3,4] with the stau [5], fine-tunings are required. In the low reheating temperature scenario, the binolike LSP can be consistent with the observed DM density without fine-tunings in the mass spectrum. For SUSY particles with masses of $O(1)$ TeV, the elestic scattering cross section between the binolike LSP and nucleon is as large as $10^{-46} - 10^{-45}{\rm cm}^2$, which is detectable in future direct detection experiments of DM such as XENON1T [67].

V. CONCLUSIONS

We have considered WIMP DM in a scenario with low reheating temperature. Although there are several mechanisms to produce DM in this scenario, including thermal production and production in a shower from the decay of the inflaton, the DM production by inelastic scatterings between high-energy particles and the thermal plasma gives the dominant contribution when the mass of the inflaton is sufficiently large. We have found that the abundance of DM depends mainly on the mass scale of the DM sector and the temperature of reheating, but not on the mass of the inflaton as long as the mass is sufficiently large. We have also found that the observed DM abundance can be accounted for when DM is heavier than $O(100)$ GeV. This conclusion is highly independent of the branching ratio of the inflaton as long as it decays into standard model particles since high-energy particles split into a lot of particles throughout inelastic scattering processes and the information of the initial condition is lost.

The above scenario is related to some cosmological topics. For example, the recent observation of high-energy cosmic-ray neutrinos by the IceCube experiment may indicate that DM is a long-lived particle with a mass of $O(1)$ PeV. The above scenario for nonthermal production of DM can also account for the abundance of even such heavy DM. In addition, since DM is produced nonthermally after the time of DM decoupling, it might have a cosmologically relevant free-streaming velocity. If

interactions between DM and the thermal plasma are irrelevant after the DM production, the present-day free-streaming velocity of DM is nonzero and would be detected by future observations of the redshifted 21-cm line.

ACKNOWLEDGMENTS

This work is supported by Grant-in-Aid for Scientific research from the Ministry of Education, Science, Sports, and Culture (MEXT), Japan, No. 25400248 (M. K.), No. 21111006 (M. K.); the World Premier International Research Center Initiative (WPI Initiative), MEXT, Japan (K. H., M. K., and M. Y.); the Program for Leading Graduate Schools, MEXT, Japan (M. Y.); and JSPS Research Fellowships for Young Scientists (K. H., K. M., and M. Y.).

APPENDIX: BOLTZMANN EQUATION DESCRIBING SPLITTINGS AND ITS STABLE SOLUTION

In this Appendix, we solve the Boltzmann equation describing splitting processes and justify the estimation of the number density of DM in Sec. III C. Let us consider a system that consists of radiation, the inflaton, and DM. In splitting processes, perpendicular momenta of daughter particles are negligible. Therefore, it is convenient to consider a momentum distribution function $\tilde{f}(p,t)$ reduced to one dimension, such that the number density is given by $n(t) = \int \mathrm{d}p \tilde{f}(p,t)$.

The Boltzmann equation, which controls splitting processes, is written as

$$\frac{\partial}{\partial t}\tilde{f}_{\mathrm{SM}}(p,t) - 3Hp\frac{\partial}{\partial p}\tilde{f}_{\mathrm{SM}}(p,t) = \frac{\mathrm{d}\Gamma_\phi}{\mathrm{d}p}n_\phi(t) + (\text{collision term}), \tag{A1}$$

where $\tilde{f}_{\mathrm{SM}}$ is the momentum distribution of the radiation and

$$n_\phi(t) = n_\phi(0)\left(\frac{a(0)}{a(t)}\right)^3 e^{-\Gamma_\phi t} \tag{A2}$$

$$\frac{\mathrm{d}\Gamma_\phi}{\mathrm{d}p} = 2\Gamma_\phi\delta(p - m_\phi/2) \tag{A3}$$

are the number density of the inflaton and its decay rate, respectively. The collision term is given as

$$\begin{aligned}(\text{collision term}) = &-\int_0^{p/2}\mathrm{d}k\frac{\mathrm{d}\Gamma_{\mathrm{split}}}{\mathrm{d}k}(k)\tilde{f}_{\mathrm{SM}}(p,t)\\ &+\int_{2p}^{m_\phi/2}\mathrm{d}k\frac{\mathrm{d}\Gamma_{\mathrm{split}}}{\mathrm{d}p}(p)\tilde{f}_{\mathrm{SM}}(k,t)\\ &+\int_0^{p}\mathrm{d}k\frac{\mathrm{d}\Gamma_{\mathrm{split}}}{\mathrm{d}k}(k)\tilde{f}_{\mathrm{SM}}(p+k,t)\end{aligned} \tag{A4}$$

(see Fig. 2), where the rate of the splitting process is given by Eqs. (10) and (14). Here we write it as

$$\frac{\mathrm{d}\Gamma_{\mathrm{split}}}{\mathrm{d}k}(k) = -\frac{1}{2}Ak^{-3/2}, \tag{A5}$$

$$A \equiv k^{1/2}\Gamma_{\mathrm{split}}(k) = (\text{const.}). \tag{A6}$$

In the above collision terms, we neglect the back reaction coming from the DM sector because the reaction rate of DM production is much smaller than that of splitting into the radiation itself.

When there is a hierarchy among time scales,

$$\Gamma_\phi \lesssim H \ll \Gamma_{\mathrm{split}}, \tag{A7}$$

which is the case of our interest in this paper, the Boltzmann equation (A1) can be solved in the following way. Since the time scale of the Hubble expansion is much longer than that of the splitting process, the second term of the left-hand side of Eq. (A1) is negligible. Further, since Standard model particles are continuously supplied by the decay of the inflaton and immediately participate in splitting processes, $\tilde{f}_{\mathrm{SM}}$ becomes a constant in time (up to a slow variation due to the red shift of the source term) as long as the source term is present, that is, $\Gamma_\phi \lesssim t^{-1} \sim H$. Then, the Boltzmann equation is reduced to the following equation:

$$\begin{aligned}0 &= -\frac{1}{2}A\left[\int_0^{p/2}\frac{\mathrm{d}k}{k^{3/2}}\tilde{f}_{\mathrm{SM}}(p) - \int_{2p}^{m_\phi/2}\frac{\mathrm{d}k}{p^{3/2}}\tilde{f}_{\mathrm{SM}}(k) - \int_0^{p}\frac{\mathrm{d}k}{k^{3/2}}\tilde{f}_{\mathrm{SM}}(p+k)\right] \quad \text{for } p < m_\phi/4,\\ 2n_\phi\Gamma_\phi\delta(p - m_\phi/2) &= \frac{1}{2}A\left[\int_0^{p/2}\frac{\mathrm{d}k}{k^{3/2}}\tilde{f}_{\mathrm{SM}}(p) - \int_0^{m_\phi/2-p}\frac{\mathrm{d}k}{k^{3/2}}\tilde{f}_{\mathrm{SM}}(p+k)\right] \quad \text{for } p > m_\phi/4.\end{aligned} \tag{A8}$$

Let us focus on the momentum distribution for $p \ll m_\phi$ and make an ansatz $\tilde{f}_{\mathrm{SM}}(p) \propto p^{-n}$. The equation is then reduced to

$$0 = -\int_0^{p/2}\frac{\mathrm{d}k}{k^{3/2}}p^{-n} + \int_{2p}^{m_\phi/2}\frac{\mathrm{d}k}{p^{3/2}}k^{-n} + \int_0^{p}\frac{\mathrm{d}k}{k^{3/2}}(p+k)^{-n}. \tag{A9}$$

This can be rewritten as

$$\frac{1}{-n+1}\left(\left(\frac{m_\phi}{2p}\right)^{-n+1}-2^{-n+1}\right) + 2\sqrt{2}+iB_{-1}\left(-\frac{1}{2},1-n\right)=0, \tag{A10}$$

$$2\sqrt{2}+iB_{-1}\left(-\frac{1}{2},1-n\right) = \int_0^1 \frac{\mathrm{d}x}{x^{3/2}}(1+x)^{-n}-\int_0^{1/2}\frac{\mathrm{d}x}{x^{3/2}}, \tag{A11}$$

where B is an incomplete beta function and i is the imaginary unit. Although the integrals in the second line have infrared divergence, the sum of them is finite. This relation implies $n=3/2$ for $p/m_\phi \ll 1$, that is,

$$\tilde{f}_{\mathrm{SM}}(p) \simeq \frac{n_\phi \Gamma_\phi}{A} m_\phi p^{-3/2}, \tag{A12}$$

where we include the coefficient $n_\phi\Gamma_\phi/A$ since the source term is proportional to this factor [see Eq. (A8)]. We also include a factor of m_ϕ by dimensional analysis.

To verify this result, let us confirm the conservation of energy in the following way. The distribution function $\tilde{f}_{\mathrm{SM}}(p)$ represents the distribution of particles that is produced from the source and evolves through inelastic scattering during the time of $O(1/\Gamma_{\mathrm{split}})$. Thus, what we should calculate in order to confirm the conservation of energy is the time integral of the source term and the momentum integral of the distribution function:

$$\int_{t_0}^{t_0+1/\Gamma_{\mathrm{split}}} \mathrm{d}t m_\phi n_\phi \Gamma_\phi \leftrightarrow \int_0^{m_\phi/2} \mathrm{d}p\, p \tilde{f}_{\mathrm{SM}}(p), \tag{A13}$$

where $t_0 (< 1/\Gamma_\phi)$ is an arbitrary time. The left-hand side is the total energy produced by inflaton decay during $t_0 < t < t_0 + 1/\Gamma_{\mathrm{split}}$, and the right-hand side is the total energy of radiation that evolves during the time of $O(1/\Gamma_{\mathrm{split}})$. These integrals are both calculated as

$$\frac{m_\phi n_\phi \Gamma_\phi}{\Gamma_{\mathrm{split}}}, \tag{A14}$$

and this result indicates the conservation of energy. However, we should note that this stable solution violates the conservation of energy for longer time span ($\gg 1/\Gamma_{\mathrm{split}}$) since the energy flows into the thermal plasma after the time of $O(1/\Gamma_{\mathrm{split}})$.

We now consider the DM production process. DM is produced from high-energy particles with energy larger than E_{th}, and the rate of the production process is given as Γ_{DM}. Thus, the number density of DM is calculated as

$$\begin{aligned} n_{\mathrm{DM}}(t) &\sim \int_{E_{\mathrm{th}}}^{m_\phi/2} \mathrm{d}p \tilde{f}_{\mathrm{SM}}(p)\Gamma_{\mathrm{DM}} t \\ &\sim n_\phi \Gamma_\phi t \frac{\Gamma_{\mathrm{DM}} m_\phi}{A E_{\mathrm{th}}^{1/2}} \\ &\sim n_\phi \Gamma_\phi t \frac{\Gamma_{\mathrm{DM}}}{\Gamma_{\mathrm{split}}(E_{\mathrm{th}})}\frac{m_\phi}{E_{\mathrm{th}}}. \end{aligned} \tag{A15}$$

Let us assume that the DM production becomes inefficient at a time t_e, which is given by kinematics [$m_\phi T(t_e) \sim m_{\mathrm{DM}}^2$] or the disappearance of the source ($t_e \sim \Gamma_\phi^{-1}$). Since the ratio of the production rate of DM to the total reaction rate is given as

$$\frac{\Gamma_{\mathrm{DM}}}{\Gamma_{\mathrm{split}}} \sim \frac{\alpha_{\mathrm{DM}}^2 T^3}{m_{\mathrm{DM}}^2}\frac{\sqrt{E_{\mathrm{th}}}}{\alpha^2 T\sqrt{T}}, \tag{A16}$$

we conclude that the energy density of DM is given by

$$\frac{\rho_{\mathrm{DM}}}{s} \sim m_{\mathrm{DM}} \frac{\alpha_{\mathrm{DM}}^2 T^3}{m_{\mathrm{DM}}^2}\frac{\sqrt{E_{\mathrm{th}}}}{\alpha^2 T\sqrt{T}}\frac{m_\phi}{E_{\mathrm{th}}}\Gamma_\phi t_e \times \frac{n_\phi}{s}, \tag{A17}$$

where we divide the energy density by the entropy density, s. The ratio n_ϕ/s should be estimated at the reheating. This result justifies Eq. (47).

[1] G. Aad *et al.* (ATLAS Collaboration), Phys. Lett. B **716**, 1 (2012).
[2] S. Chatrchyan *et al.* (CMS Collaboration), Phys. Lett. B **716**, 30 (2012).
[3] K. Griest and D. Seckel, Phys. Rev. D **43**, 3191 (1991).
[4] P. Gondolo and G. Gelmini, Nucl. Phys. **B360**, 145 (1991).
[5] J. R. Ellis, T. Falk, and K. A. Olive, Phys. Lett. B **444**, 367 (1998).
[6] M. Ibe, T. Moroi, and T. T. Yanagida, Phys. Lett. B **644**, 355 (2007); M. Ibe and T. T. Yanagida, Phys. Lett. B **709**, 374 (2012); M. Ibe, S. Matsumoto, and T. T. Yanagida, Phys. Rev. D **85**, 095011 (2012).
[7] J. L. Feng, K. T. Matchev, and D. Sanford, Phys. Rev. D **85**, 075007 (2012).
[8] N. Okada, arXiv:1205.5826.
[9] J. L. Feng, Z. Surujon, and H. -B. Yu, Phys. Rev. D **86**, 035003 (2012).

[10] N. Arkani-Hamed, A. Gupta, D. E. Kaplan, N. Weiner, and T. Zorawski, arXiv:1212.6971.
[11] T. T. Yanagida and N. Yokozaki, Phys. Lett. B **722**, 355 (2013); J. High Energy Phys. 11 (2013) 020.
[12] D. J. H. Chung, E. W. Kolb, and A. Riotto, Phys. Rev. D **60**, 063504 (1999).
[13] G. F. Giudice, E. W. Kolb, and A. Riotto, Phys. Rev. D **64**, 023508 (2001).
[14] T. Moroi, M. Yamaguchi, and T. Yanagida, Phys. Lett. B **342**, 105 (1995).
[15] M. Kawasaki, T. Moroi, and T. Yanagida, Phys. Lett. B **370**, 52 (1996).
[16] T. Moroi and L. Randall, Nucl. Phys. **B570**, 455 (2000).
[17] G. B. Gelmini and P. Gondolo, Phys. Rev. D **74**, 023510 (2006).
[18] Y. Kurata and N. Maekawa, Prog. Theor. Phys. **127**, 657 (2012).
[19] R. Allahverdi and M. Drees, Phys. Rev. Lett. **89**, 091302 (2002); R. Allahverdi and M. Drees, Phys. Rev. D **66**, 063513 (2002).
[20] S. Sarkar and R. Toldra, Nucl. Phys. **B621**, 495 (2002); R. Toldra, Comput. Phys. Commun. **143**, 287 (2002).
[21] C. Barbot and M. Drees, Phys. Lett. B **533**, 107 (2002); Astropart. Phys. **20**, 5 (2003); C. Barbot, Comput. Phys. Commun. **157**, 63 (2004).
[22] A. Kurkela and G. D. Moore, J. High Energy Phys. 12 (2011) 044.
[23] K. Harigaya and K. Mukaida, arXiv:1312.3097.
[24] S. Davidson and S. Sarkar, J. High Energy Phys. 11 (2000) 012.
[25] P. B. Arnold, G. D. Moore, and L. G. Yaffe, J. High Energy Phys. 01 (2003) 030.
[26] P. Jaikumar and A. Mazumdar, Nucl. Phys. **B683**, 264 (2004).
[27] L. D. Landau and I. Pomeranchuk, Dokl. Akad. Nauk SSSR. **92**, 535 (1953).
[28] A. B. Migdal, Phys. Rev. **103**, 1811 (1956).
[29] M. Gyulassy and X.-N. Wang, Nucl. Phys. **B420**, 583 (1994).
[30] P. B. Arnold, G. D. Moore and L. G. Yaffe, J. High Energy Phys. 11 (2001) 057.
[31] P. B. Arnold, G. D. Moore, and L. G. Yaffe, J. High Energy Phys. 12 (2001) 009.
[32] P. B. Arnold, G. D. Moore, and L. G. Yaffe, J. High Energy Phys. 06 (2002) 030.
[33] D. Besak and D. Bodeker, J. High Energy Phys. 05 (2010) 007.
[34] K. Griest and M. Kamionkowski, Phys. Rev. Lett. **64**, 615 (1990).
[35] M. G. Aartsen *et al.* (IceCube Collaboration), Science **342**, 1242856 (2013).
[36] B. Feldstein, A. Kusenko, S. Matsumoto, and T. T. Yanagida, Phys. Rev. D **88**, 015004 (2013).
[37] A. Esmaili and P. D. Serpico, J. Cosmol. Astropart. Phys. 11 (2013) 054.
[38] Y. Bai, R. Lu, and J. Salvado, arXiv:1311.5864.
[39] T. Moroi, H. Murayama, and M. Yamaguchi, Phys. Lett. B **303**, 289 (1993).
[40] M. Bolz, A. Brandenburg, and W. Buchmuller, Nucl. Phys. **B606**, 518 (2001); M. Bolz, A. Brandenburg, and W. BuchmullerNucl. Phys. **B790**, 336 (2008).
[41] J. Pradler and F. D. Steffen, Phys. Rev. D **75**, 023509 (2007).
[42] A. Kusenko, F. Takahashi, and T. T. Yanagida, Phys. Lett. B **693**, 144 (2010).
[43] Y. Mambrini, K. A. Olive, J. Quevillon, and B. Zaldivar, Phys. Rev. Lett. **110**, 241306 (2013).
[44] P. A. R. Ade *et al.* (Planck Collaboration), arXiv:1303.5076.
[45] M. Fujii and K. Hamaguchi, Phys. Lett. B **525**, 143 (2002); Phys. Rev. D **66**, 083501 (2002).
[46] S. Dimopoulos, G. R. Dvali, and R. Rattazzi, Phys. Lett. B **410**, 119 (1997).
[47] F. Takahashi, Phys. Lett. B **693**, 140 (2010); K. Nakayama and F. Takahashi, J. Cosmol. Astropart. Phys. 11 (2010) 009.
[48] K. Harigaya, M. Ibe, K. Schmitz, and T. T. Yanagida, Phys. Lett. B **720**, 125 (2013).
[49] K. Enqvist and J. McDonald, Phys. Lett. B **425**, 309 (1998); Nucl. Phys. **B538**, 321 (1999).
[50] M. Fujii and T. Yanagida, Phys. Lett. B **542**, 80 (2002).
[51] A. Kamada, M. Kawasaki, and M. Yamada, Phys. Lett. B **719**, 9 (2013).
[52] R. D. Peccei and H. R. Quinn, Phys. Rev. Lett. **38**, 1440 (1977); Phys. Rev. D **16**, 1791 (1977); S. Weinberg, Phys. Rev. Lett. **40**, 223 (1978); F. Wilczek, Phys. Rev. Lett. **40**, 279 (1978).
[53] M. Viel, G. D. Becker, J. S. Bolton, and M. G. Haehnelt, Phys. Rev. D **88**, 043502 (2013).
[54] F. D. Steffen, J. Cosmol. Astropart. Phys. 09 (2006) 001.
[55] M. Sitwell, A. Mesinger, Y.-Z. Ma, and K. Sigurdson, arXiv:1310.0029.
[56] J. Hisano, K. Kohri, and M. M. Nojiri, Phys. Lett. B **505**, 169 (2001).
[57] G. Arcadi and P. Ullio, Phys. Rev. D **84**, 043520 (2011).
[58] M. Ibe, A. Kamada, and S. Matsumoto, Phys. Rev. D **87**, 063511 (2013).
[59] I. Affleck and M. Dine, Nucl. Phys. **B249**, 361 (1985).
[60] M. Dine, L. Randall, and S. D. Thomas, Nucl. Phys. **B458**, 291 (1996).
[61] K. Enqvist and J. McDonald, Phys. Rev. Lett. **83**, 2510 (1999).
[62] K. Enqvist and J. McDonald, Phys. Rev. D **62**, 043502 (2000).
[63] M. Kawasaki and F. Takahashi, Phys. Lett. B **516**, 388 (2001).
[64] S. Kasuya, M. Kawasaki, and F. Takahashi, J. Cosmol. Astropart. Phys. 10 (2008) 017.
[65] G. Hinshaw *et al.* (WMAP Collaboration), Astrophys. J. Suppl. Ser. **208**, 19 (2013).
[66] P. A. R. Ade *et al.* (Planck Collaboration), arXiv:1303.5082.
[67] E. Aprile (XENON1T Collaboration) arXiv:1206.6288.